The Astrophysical Journal, 952:173 (4pp), 2023 August 1 https://doi.org/10.3847/1538-4357/ace691

Erratum: "Modeling the Thermodynamic Evolution of Coronal Mass Ejections Using Their Kinematics" (2018, ApJ, 865, 50)

Wageesh Mishra[1], Yuming Wang[2], Shaoyu Lyu[2], and Soumyaranjan Khuntia[1]
[1] Indian Institute of Astrophysics, II Block, Koramangala, Bengaluru 560034, India; wageesh.mishra@iiap.res.in
[2] CAS Key Laboratory of Geospace Environment, Department of Geophysics and Planetary Sciences, University of Science and Technology of China, Hefei 230026, People's Republic of China; ymwang@ustc.edu.cn
Received 2023 July 6; published 2023 August 3

In the published article (hereafter referred to as Paper I), we improved a self-similar flux-rope internal state (FRIS) model for understanding the evolution of various internal dynamic (Lorentz, thermal, and centrifugal forces) and thermodynamic parameters (polytropic index, heating rate, etc.) of a coronal mass ejection (CME). We implemented the FRIS model to a CME that occurred on 2008 December 12. Although the physical basis and methods of building the analytical FRIS model have no errors in Paper I, we recently discovered an initial miscalculation in the expression of the Lorentz force (Equation (23) in Paper I), resulting in systematic errors in calculating several other parameters. The miscalculation did not significantly alter the general trends of the derived internal state parameters of the CME but affected the absolute or scaled magnitude of the derived parameters. In this erratum, we present a detailed account of the modifications made in the equations. We redo the analysis keeping our methodology exactly the same as in Paper I and provide updated figures of the derived dynamic and thermodynamic parameters.

With corrections incorporated, the notable changes in the equations of Paper I are as follows.

Equation (23) of Paper I will be revised as

$$\overline{f}_{\rm em} = \frac{k_2 M a_e}{lR^2} - \frac{k_1^2 k_3 L_A^2}{MlR^5} - \frac{k_4 M^\gamma e^{\sigma s}}{l^\gamma R^{2\gamma+1}}.$$

Equation (24) will be revised as

$$\overline{f}_{\rm th} = \frac{k_4 M^\gamma e^{\sigma s}}{l^\gamma R^{2\gamma+1}}.$$

Equation (30) will be revised as

$$a_e - c_1 R^{-3} = c_2 L R^{-3} + c_3 L^{-1} R^{-1} + \lambda(t) L^{1-\gamma} R^{1-2\gamma}.$$

Equation (34) will be revised as

$$\bar{f}_{\rm th} = \frac{k_4 M^\gamma e^{\sigma s}}{l^\gamma R^{2\gamma+1}} = \frac{k_2 M}{k_7}[\lambda(t) L^{-\gamma} R^{-2\gamma-1}].$$

Equation (46) will be revised as

$$\lambda(t) = L^{\gamma-1} R^{2\gamma-1}(a_e - c_1 R^{-3} - c_2 L R^{-3} - c_3 L^{-1} R^{-1}).$$

Equation (47) will be revised as

$$\begin{aligned}\frac{d\lambda}{dt} = L^{\gamma-1} R^{2\gamma-1}\Bigg[&\left(\frac{da_e}{dt} + (2\gamma-1) a_e v_e R^{-1} + (\gamma-1) a_e v_c L^{-1}\right)\\ &+ c_1((4-2\gamma) v_e R^{-4} + (1-\gamma) v_c L^{-1} R^{-3})\\ &+ c_2((4-2\gamma) v_e L R^{-4} - \gamma v_c R^{-3})\\ &+ c_3((2-2\gamma) v_e L^{-1} R^{-2} + (2-\gamma) v_c L^{-2} R^{-1})\Bigg].\end{aligned}$$

Equation (49) will be revised as

$$(LR^2)^{\gamma-1} = c_4 L R^{-2} \frac{d\lambda}{dt} + c_5 \lambda.$$

Table 1
List of the Derived Internal Thermodynamic Parameters from the FRIS Model

Quantities	Factors	Values	SI Units
Lorentz force ($\bar{f}_{\rm em}$)	$\frac{k_2 M}{k_7}$	$c_2 R^{-5} + c_3 L^{-2} R^{-3}$	Pa m^{-1}
Thermal pressure force ($\bar{f}_{\rm th}$)	$\frac{k_2 M}{k_7}$	$\lambda(t) L^{-\gamma} R^{-2\,\gamma-1}$	Pa m^{-1}
Centrifugal force ($\bar{f}_p$)	$\frac{k_2 M}{k_7}$	$c_1 R^{-5} L^{-1}$	Pa m^{-1}
Proton number density ($\bar{n}_p$)	$\frac{M}{k_7}$	$\frac{1}{\pi m_p}(LR^2)^{-1}$	m^{-3}
Thermal pressure ($\bar{p}$)	$\frac{k_2 k_8 M}{k_4 k_7}$	$\lambda (LR^2)^{-\gamma}$	Pa
Temperature ($\bar{T}$)	$\frac{k_2 k_8}{k_4}$	$\frac{\pi\sigma}{(\gamma-1)}\lambda (LR^2)^{1-\gamma}$	K
Rate of change of entropy ($\frac{d\bar{s}}{dt}$)		$\frac{1}{\sigma\lambda}\frac{d\lambda}{dt}$	J K^{-1} kg^{-1} s^{-1}
Heating rate ($\bar{\kappa}$)	$\frac{k_2 k_8}{k_4}$	$\frac{\pi}{(\gamma-1)}(LR^2)^{1-\gamma}\frac{d\lambda}{dt}$	J kg^{-1} s^{-1}
Thermal energy (E_i)	$\frac{k_2 k_8 M}{k_4}$	$\frac{\pi}{(\gamma-1)}(LR^2)^{1-\gamma}\lambda$	J
Magnetic energy (E_m)		$E_{m1} + E_{m2}$	J
E_{m1}	$\frac{k_9}{k_7}$	$\frac{\pi L^{-1}}{\mu_0}$	J
E_{m2}	$k_7 k_{10}$	$\frac{\pi L R^{-2}}{\mu_0}$	J
Polytropic Index (Γ)		$\gamma + \frac{\ln\frac{\lambda(t)}{\lambda(t+\Delta t)}}{\ln\left[\left(\frac{L(t+\Delta t)}{L(t)}\right)\left[\frac{R(t+\Delta t)}{R(t)}\right]^2\right]}$	

Note. The details of coefficients (c_{1-5}) and factors are the same as in Table 1 of Paper I.

Equation (52) will be revised as

$$(LR^2)^{\gamma-1} = L^{\gamma-1}R^{2\gamma-1}\Bigg[\Bigg(c_5 a_e - c_3 c_5 L^{-1}R^{-1} + (c_4 L\frac{da_e}{dt} + (\gamma-1)c_4 a_e v_c)R^{-2}\Bigg) + ((2-\gamma)c_3 c_4 v_c L^{-1} + (2\gamma-1)c_4 a_e v_e L - c_2 c_5 L - c_1 c_5)R^{-3} + ((2-2\gamma)c_3 c_4 v_e)R^{-4} + ((1-\gamma)c_1 c_4 v_c - \gamma c_2 c_4 v_c L)R^{-5} + ((4-2\gamma)c_1 c_4 v_e L + (4-2\gamma)c_2 c_4 v_e L^2)R^{-6}\Bigg].$$

Rearranging the above equation, we can write it further as the following:

$$\frac{R}{L} = c_5\left[\frac{a_e R^2}{L}\right] - c_3 c_5\left[\frac{R}{L^2}\right] - c_2 c_5\left[\frac{1}{R}\right] - c_1 c_5\left[\frac{1}{LR}\right] + c_4\left[\frac{da_e}{dt} + \frac{(\gamma-1)a_e v_c}{L} + \frac{(2\gamma-1)a_e v_e}{R}\right] + c_3 c_4\left[\frac{(2-\gamma)v_c}{L^2 R} + \frac{(2-2\gamma)v_e}{LR^2}\right] + c_2 c_4\left[\frac{(4-2\gamma)v_e L}{R^4} - \frac{\gamma v_c}{R^3}\right] + c_1 c_4\left[\frac{(4-2\gamma)v_e}{R^4} + \frac{(1-\gamma)v_c}{LR^3}\right]. \quad (1)$$

On correcting the miscalculations as above, the expressions for FRIS model-derived output parameters will also be modified, which are listed in Table 1.

We reanalyze the 2008 December 12 CME case study and follow the methodology described in Section 3.2 of Paper I. The fitting of the measured R/L in the left-hand side of Equation (1) with the model-derived expression as in the right-hand side of the equation is done to find the best set of unknown model fitting coefficients (c_{1-5}). The goodness of fit is shown in the top-left panel of Figure 1. Using the fitted coefficients and measured kinematic parameters in the expressions for different dynamic and thermodynamic parameters as listed in Table 1, we estimate the updated values of internal state parameters of the CME during its evolution in the corona.

In the updated results, the most noticeable change is in the evolution of the polytropic index (Γ) as shown in the top-right panel of Figure 1. The earlier finding (top-left panel of Figure 5 in Paper I) of a decrease in the value of Γ from 1.8 to 1.37 as the heliocentric distance (D) of the center of CMEs increased from 5.8 to 13.6 $R_\odot$ is no longer valid. The corrected value of Γ still maintains a gradual decrease, but now it changes only from 1.32 to 0.98 for $D = 5.8$ to 13.6 $R_\odot$. The corrected value does not show the transition of the CME from heat release to heat-absorption state; instead, the CME consistently remains in a heat-absorption state throughout its propagation in the corona.

The earlier finding (Figure 6 of Paper I) that CME had negative values of heating rate ($\kappa = dQ/dt$) and rate of change of entropy (ds/dt) in the beginning, and then its value increased to positive values is no longer valid. Therefore, the earlier discussion that the

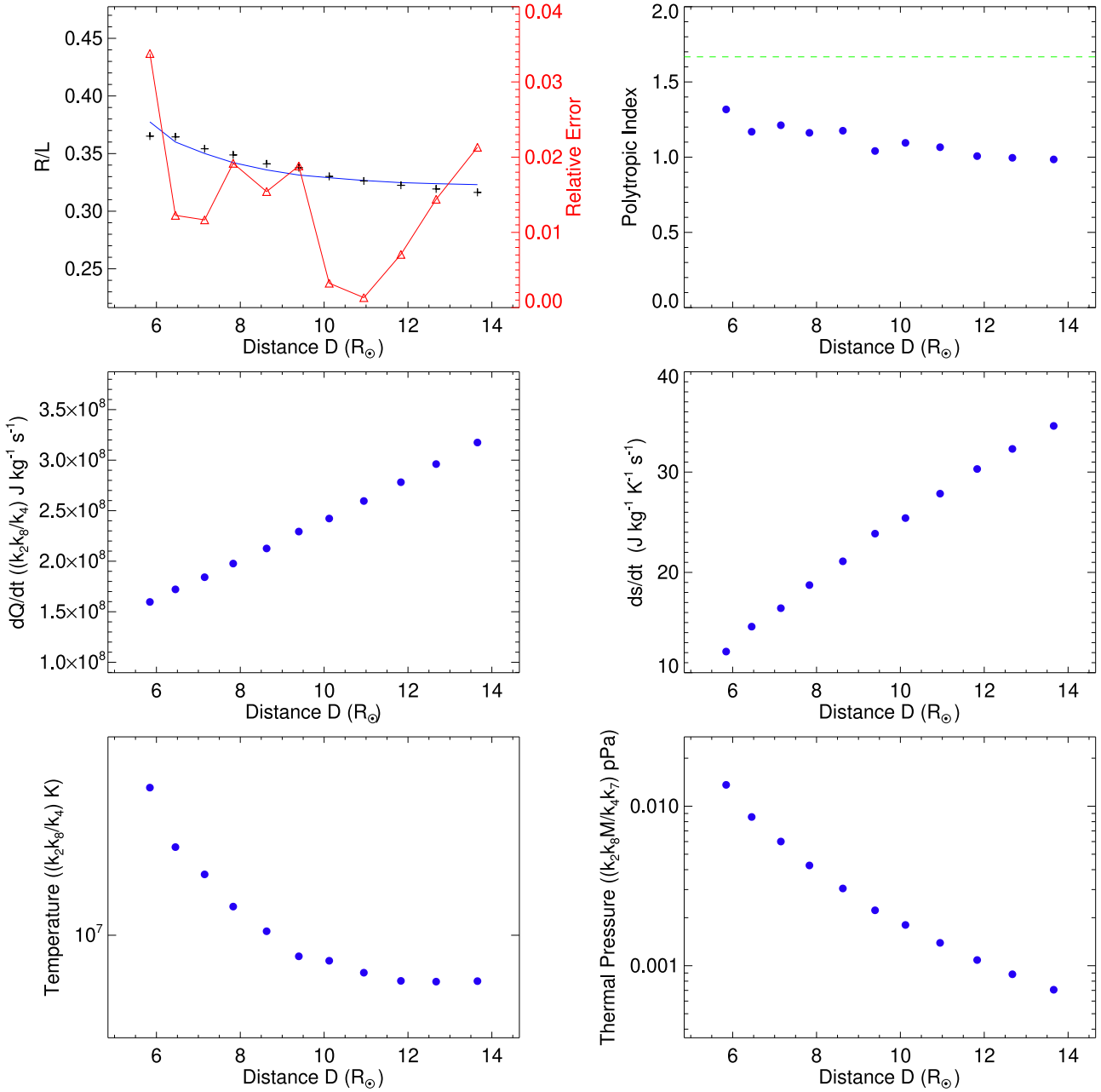

Figure 1. The goodness of fit for Equation (1) is shown in the top-left panel. The variation in the polytropic index, heating rate, rate of change of entropy, temperature, and thermal pressure with the heliocentric distance (D) of CME's center is shown in the top-right, middle-left, middle-right, bottom-left, and bottom-right panels, respectively.

CME was initially heat-releasing before transitioning to an adiabatic state at $D = 9\ R_\odot$, eventually entering a heat-absorption state, is incorrect. Thus, all parameters depicted in Figure 6 of Paper I no longer demonstrate a transition from negative to positive values. The updated results show a continual injection of heat into the CME plasma throughout the range of $D = 5.8$ to 13.6 $R_\odot$, leading to persistently positive values for both the heating rate and the rate of entropy change, as illustrated in the middle-left and middle-right panels of Figure 1, respectively. Although the updated profile of CME temperature (bottom-left panel of Figure 1) shows a decreasing trend, it is not as steep as previously reported in the bottom-left panel of Figure 5 in Paper I. This finding is consistent with the corrected values of the polytropic index. We did not find any change in the estimated density profile of the CME; however, the thermal pressure values are updated as depicted in the bottom-right panel of Figure 1.

The updated values of different forces and their relative magnitude are shown in Figure 2. It is important to note that the corrections made did not significantly change the magnitudes of the Lorentz and thermal pressure forces. However, the magnitude of the centrifugal force was indeed affected. Although the centrifugal force was smaller than the other two forces in Paper I, its corrected values decreased further, making it relatively insignificant compared to the other forces. Consequently, the magnitude and direction of the net force (bottom-right panel of Figure 2) remain unaffected by the corrections made in the FRIS model. Our earlier finding is that the centrifugal force decreases fastest among the three forces, and the Lorentz force decreases slightly faster than the thermal

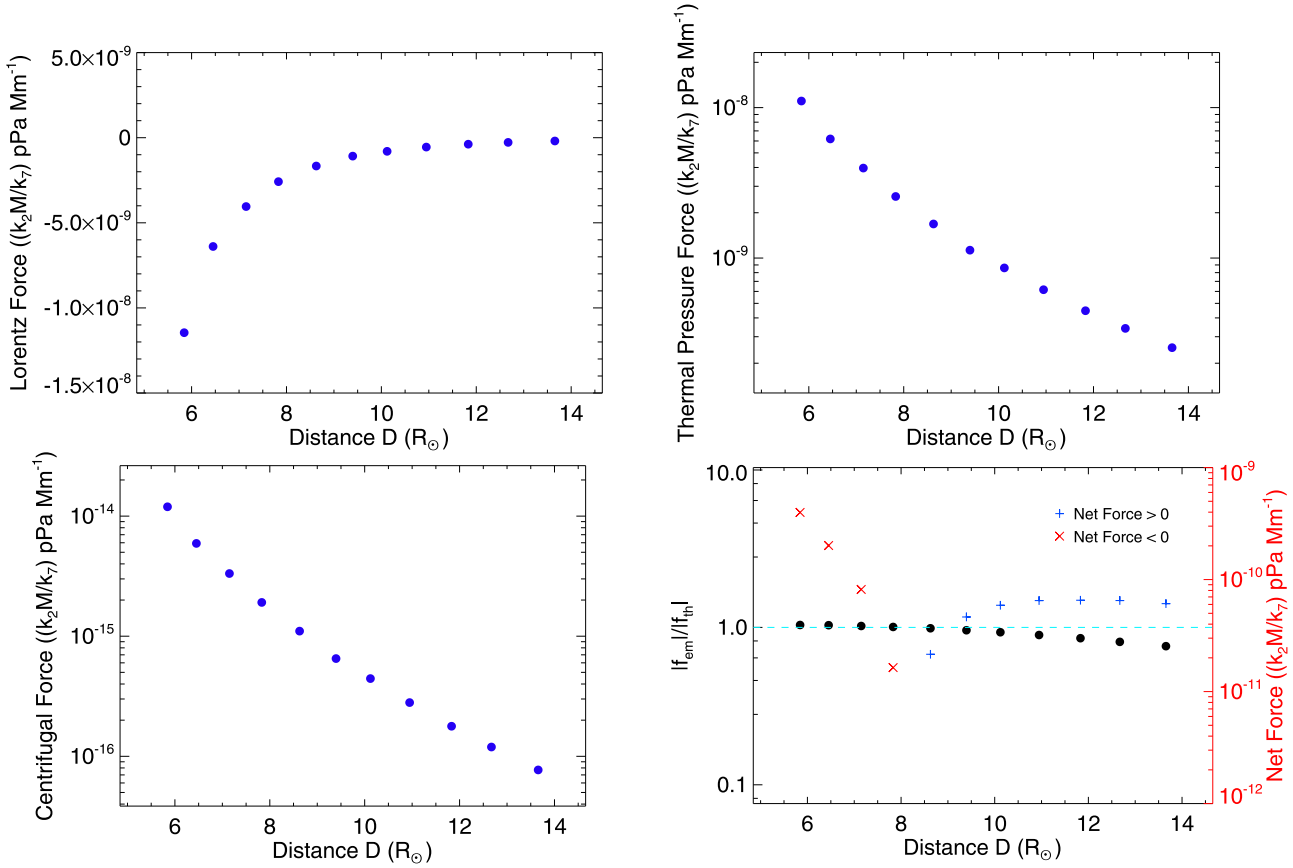

Figure 2. The evolution of average Lorentz force ($\bar{f}_{em}$), thermal pressure force ($\bar{f}_{th}$), and centrifugal force ($\bar{f}_{p}$) acting on the CME with the heliocentric distance of its center (D) are shown in the top-left, top-right, and bottom-left panels, respectively. The ratio of the absolute values of the Lorentz and thermal forces (on the left Y-axis), as well as the net force (on the right Y-axis) acting inside the CME, is shown in the bottom-right panel.

pressure force remains unchanged. Furthermore, the finding regarding the outward direction of the thermal pressure and centrifugal forces from the center of the CME, while the Lorentz force acts inward, also remains unchanged.

In summary, the corrections applied to the FRIS model do not alter the overall conclusions regarding the decreasing trends observed in density, temperature, thermal pressure, and the forces (Lorentz, thermal, and centrifugal) acting on the evolving CME. However, the correction primarily influences our findings (Section 3.3 of Paper I) on the transition of the polytropic index, heating rate, and rate of change of entropy of the CME from heat-releasing to heat-absorption state. Nonetheless, the general discussion presented in Section 4 of Paper I about the advantages and limitations of the FRIS model remains unchanged.

ORCID iDs

Wageesh Mishra https://orcid.org/0000-0003-2740-2280
Yuming Wang https://orcid.org/0000-0002-8887-3919
Shaoyu Lyu https://orcid.org/0000-0002-2349-7940
Soumyaranjan Khuntia https://orcid.org/0009-0006-3209-658X